McGill University

The Bosonic Kitaev Chain

Alexander McDonald

Department of Physics

August 2018

McGill University, Montreal, Quebec

A thesis submitted to McGill University in partial fulfillment of the requirements of the degree of Master of Science

Abstract

Majorana fermions have garnered a large amount of attention in recent years due to their unusual behavior. They are intimately related to the exotic phenomena of topological superconductivity and consequently lie at the heart of all current proposals for topological quantum computers. Perhaps the simplest model which realizes the necessary physics required for such computers is the fermionic Kitaev chain model. A natural question to ask is whether the same physics can be realized for photons, which unlike electrons, are bosons and not fermions. In this thesis, we introduce and study a bosonic version of the Kitaev chain. Much like the original fermionic version, we show that the model is best understood in terms of the local Hermitian degrees of freedom. The system demonstrates phase-dependent chirality; signals propagate and are amplified in a manner which depends on the *phase* of the photonic excitation. Further, we find a striking sensitivity to boundary conditions: the boundary-less system is characterized by delocalized dynamically stable modes whereas the finite system with open boundaries only supports localized, stable modes. Finally, we discuss our system's entanglement properties. While we focus specifically on a photonic system, our ideas are in principle applicable to any kind of bosonic system.

Résumé

Les fermions de Majorana ont attiré beaucoup d'attention ces dernières années du à leur comportement inhabituel. Ils sont intimement liés aux phénomènes exotiques de supraconductivité topologique et sont donc au coeur de toutes les propositions actuelles pour les ordinateurs quantiques topologiques. Peut-être le modèle le plus simple qui réalise la physique nécessaire pour de tels ordinateurs est la chaîne fermionique de Kitaev. Une question naturelle à se poser est de savoir si la même physique peut être réalisée pour les photons, qui contrairement aux électrons, sont des bosons et non des fermions. Dans cette thèse, nous présentons et étudions une version bosonique de la chaîne de Kitaev. Toute comme la version fermionique originale, nous montrons que le modèle est mieux compris en termes de degrés de liberté hermitiens locaux. Le système démontre une chiralité qui dépant de la *phase*; les signaux se propagent et sont amplifiés d'une manière qui dépend de la phase de l'excitation photonique. En outre, nous trouvons une sensibilité frappante aux conditions de limites: le système sans limites est caractérisé par des modes dynamiquement stables délocalisés alors que le système fini avec des frontières ouvertes ne supporte que des modes localisés et stables. Enfin, nous discutons de l'enchevêtrement de notre système. Alors que nous nous concentrons spécifiquement sur un système photonique, nos idées sont en principe applicable à tout type de système bosonique.

Acknowledgments

I would like to thank my supervisors Aash Clerk and Tami Pereg-Barnea for their continued support during my time at McGill. Their knowledge, insights, and patience have undoubtedly made me a better physicist. I would always feel comfortable asking for advice, explanations of things I didn't understand, or presenting new ideas. And while I look forward to my completing my PhD under Aash's supervision in Chicago, I am also saddened by the thought of Tami not joining our weekly meetings. Furthermore, I am grateful that they allowed me to return home to Ottawa for the second half of my degree, a particularly difficult time in my life. It meant the world to both my family and I.

Being in two groups at once gave me the opportunity to interact with two amazing groups of young scientists. In particular, I would like to thank Misha, Catherine, Luke, Martin, Rosa, Kunal, Aaron, and everyone else in Aash's and Tami's group for both their helpful discussions and comradery. Outside of those groups, I am especially grateful to Daniel, Felix and Raphël. Our discussions at lunch always brightened my day.

Outside of the Rutherford physics building, I would also like to thank Justin, Erik, JP, GB, and especially my roommate Mart, without whom my experience in Montreal would have been dull to say the least. They are my closest group of friends with whom I've had countless memories, and I know they will be for a long time to come. Finally, and most importantly, I am eternally grateful to my parents, my twin sister and my older brother. I have neither the requisite space nor eloquence to adequately describe how much they have done for me, so I will simply resort to the trite, knowing that they understand what I mean anyway. Thank you.

Contents

List of Figures

1

Introduction

Topological insulators and superconductors are relatively new states of matter which are by now extremely well understood. They are characterized by a fully insulating bulk, yet host gapless edge states. A particularly simple model in which the presence of these edge states is extremely transparent is the Kitaev chain, a topological superconductor whose edge modes are exotic states known as Majorana modes [1]. The fermionic nature of the electron is crucial to the physics displayed by the Kitaev chain. In this thesis, we will therefore attempt to answer a relatively simple if broad question; is there an interesting analogue of Kitaev chain in the bosonic case? Before diving into the question at hand, we first briefly review Kitaev's original model and a few of its remarkable properties. We then touch on the basic theory required to understand parametrically driven bosonic systems, the bosonic equivalent of superconductors. Finally, we introduce the bosonic Kitaev chain, the model that we will study throughout the rest of this thesis.

1.1 Fermionic Kitaev Chain

Before trying to study the bosonic Kitaev chain, we briefly review the original fermionic version. The purpose here is not to exhaustively study this interesting model, but rather highlight its remarkable properties. Despite several noteworthy features, the fermionic Kitaev chain is deceptively simple: it consists of spinless electrons hopping on a 1D lattice subject to a p-wave superconducting pairing amplitude, described by the Hamiltonian

$$\hat{H}_F = \frac{1}{2}\sum_j \left(t\hat{c}^\dagger_{j+1}\hat{c}_j - \mu\hat{c}^\dagger_j\hat{c}_j + i\Delta\hat{c}^\dagger_{j+1}\hat{c}^\dagger_j + h.c.\right) \tag{1.1.1}$$

where $\hat{c}_j$ and $\hat{c}^\dagger_j$ are electron creation and annihilation operators at site j, t is the hopping amplitude, μ is the chemical potential, and Δ is the superconducting pair potential. Note that the phase of Δ amounts of a choice of gauge and without loss of generality we may set $\Delta > 0$. Since the model is translationally invariant, momentum is conserved. Moving to the momentum basis, the Hamiltonian reads

$$\hat{H}_F = \sum_k \left[(t\cos k - \mu)\ \hat{c}^\dagger_k\hat{c}_k + i\frac{\Delta}{2}\sin k \left(\hat{c}^\dagger_k\hat{c}^\dagger_{-k} - h.c.\right)\right] \tag{1.1.2}$$

where $\hat{c}_k$ and $\hat{c}^\dagger_k$ annihilate and create an electron with momentum k respectively. The amplitude $i\Delta\sin k$ pairs up electrons with a zero net center of mass momentum, a consequence of translational invariance. Furthermore, due to Fermi statistics, the pairing amplitude must be an odd function of k.

The amazing properties of the Kitaev chain can be traced back to its topological origins. This is more transparent by introducing a two component operator $C^\dagger_k = (\hat{c}^\dagger_k, \hat{c}_{-k})$

and rewriting Eq.(1.1.2) as

$$\hat{H}_F = \frac{1}{2} \sum_k C_k^\dagger \left(\mathbf{h}_F(k) \cdot \check{\boldsymbol{\sigma}} \right) C_k, \tag{1.1.3}$$

where $\mathbf{h}_F(k) = (0, -\Delta \sin(k), t\cos(k) - \mu)$ and $\check{\boldsymbol{\sigma}}$ is a vector of Pauli matrices in particle-hole space. Since $h_x(k)$ is zero for all momentum, the momentum space Hamiltonian anti-commutes with the first Pauli matrix, i.e. $\check{\sigma}_x \left(\mathbf{h}_F(k) \cdot \check{\boldsymbol{\sigma}} \right) \check{\sigma}_x = -\mathbf{h}_F(k) \cdot \check{\boldsymbol{\sigma}}$. The momentum space Hamiltonian, anticommuting with a unitary operator, is then said to have chiral symmetry. Due to this symmetry, we consider $\mathbf{h}_F(k)$ as a two-dimensional vector and subsequently define a topological number which counts the number of times the vector $\mathbf{h}_F(k)$ encircles the origin. In the Kitaev chain when $\mu = 0$ (which we consider from now on),the vector $\mathbf{h}_F(k)$ encircles the origin once, indicating a topologically non-trivial state. The bulk energies are given by $E_\pm(k) = \pm|\mathbf{h}_F| = \pm\sqrt{t^2(\cos k)^2 + \Delta^2(\sin k)^2}$ which implies that this topological number can't change unless we close the bulk gap (i.e. $|\mathbf{h}_F(k)| = 0$ for some k in the Brillouin zone).

The interest in topological states of matter is not purely academic: there are interesting physical consequences to having a non-zero topological number. The quintessential example is the bulk-boundary correspondence, which in the context of topological band theory states that a topologically non-trivial system supports protected zero-energy modes at its boundary [2–4]. Having just demonstrated that the fermionic Kitaev chain has such a non-zero topological number, we know that the finite-size version with open boundary conditions must have an edge mode, which we now demonstrate. The relevant Hamiltonian is

$$\hat{H}_F = \frac{1}{2} \sum_{j=1}^{N-1} \left(t\hat{c}_{j+1}^\dagger \hat{c}_j + i\Delta \hat{c}_{j+1}^\dagger \hat{c}_j^\dagger + h.c. \right) \tag{1.1.4}$$

The existence of edge modes is most easily seen by introducing new localized degrees of freedom on each site, the Majorana operators $\hat{\gamma}_{Aj}$ and $\hat{\gamma}_{Bj}$ via

$$\hat{c}_j = \frac{e^{i\frac{\pi}{4}}}{\sqrt{2}} \left(\hat{\gamma}_{Aj} + i\hat{\gamma}_{Bj}\right). \tag{1.1.5}$$

One can easily verify that both $\hat{\gamma}_{Aj}$ an $\hat{\gamma}_{Bj}$ operators are Hermitian and satisfy the usual fermionic anticommutation relations

$$\hat{\gamma}^{\dagger}_{\alpha,j} = \hat{\gamma}_{\alpha,j} \qquad\qquad \{\hat{\gamma}_{\alpha,j}, \hat{\gamma}_{\alpha' j'}\} = \delta_{j,j'}\delta_{\alpha,\alpha'} \tag{1.1.6}$$

With that being said, asking whether a Majorana mode is occupied or not is meaningless, since $\hat{\gamma}^{\dagger}_{\alpha j}\hat{\gamma}_{\alpha,j} = \hat{\gamma}^2_{\alpha,j} = \frac{1}{2}$. Instead, these modes should be viewed as "half" a regular fermion.

Expressed in the Majorana basis, the Hamiltonian takes the form

$$\hat{H}_F = \frac{-i}{2} \sum_{j=1}^{N-1} \left(-(t-\Delta)\hat{\gamma}_{A,j+1}\hat{\gamma}_{B,j} + (t+\Delta)\hat{\gamma}_{B,j+1}\hat{\gamma}_{A,j}\right). \tag{1.1.7}$$

Thus, A-type Majoranas only couple to B-type Majorana's and vice-versa. Furthermore, the coupling between $\hat{\gamma}_{A,j}$ and $\hat{\gamma}_{B,j\pm 1}$ is asymmetric. Is it precisely this asymmetry that leads to the edge modes. This is most easily demonstrated in the limit where $\Delta = t$ and the Hamiltonian is given by

$$\hat{H}_F = -it \sum_{j=1}^{N-1} \hat{\gamma}_{B,j+1}\hat{\gamma}_{A,j} = t \sum_{j=1}^{N-1} \left(\hat{d}^{\dagger}_j \hat{d}_j - \frac{1}{2}\right). \tag{1.1.8}$$

$\hat{d}_j = \frac{1}{\sqrt{2}}(\hat{\gamma}_{A,j} + i\hat{\gamma}_{B,j+1})$ are new fermionic operators, which consists of two Majorana mode on adjacent sites. In agreement with the analysis of the bulk, we see that one must pay an energy cost of t to add a $\hat{d}_j$ fermion. However there are still two Majoranas, $\hat{\gamma}_{B,1}$

and $\hat{\gamma}_{A,N}$ which do not appear in the Hamiltonian. One can therefore define a new, highly non-local fermion $\hat{f} = \frac{1}{\sqrt{2}}(\hat{\gamma}_{A,N} + i\hat{\gamma}_{B,1})$ which costs zero energy. This zero-energy mode is completely invisible to the bulk theory, which is best understood by imposing periodic boundary conditions on our chain. In this case, the two Majoranas $\hat{\gamma}_{A,N}$ and $\hat{\gamma}_{B,1}$ are actually coupled to one another, creating an energy gap. In going from open to periodic boundary conditions, we've "split" the fermionic mode f into two, leaving a Majorana fermion at each end of the chain.

This concludes our brief review of the Kitaev chain. We've seen that the bulk system is gapped and carries a non-zero topological invariant yet, in accordance with the bulk-boundary correspondence, hosts zero-energy modes localized at its edges. We note that away from the point $\Delta = t$ in parameter space, these modes are not exactly at zero energy nor localized purely at the edges. Instead, their wavefunctions decay exponentially into the bulk and the corresponding energy decays exponentially as the length of the chain as long as the bulk is gapped [1, 2]. These localized states are still present even for a non-zero chemical potential $\mu \neq 0$ as long as the vector $\mathbf{h}_F(k)$ winds once around the origin, i.e. when $|t| > |\mu|$. Furthermore, the localization physics is best understood in terms of Majorana modes, which we can colloquially think of as "half" a fermion. It is only natural to ask whether the same physics can be realized in a bosonic system which, formally, resembles a fermionic superconductor. Before addressing this question however, we must first discuss how such models can be physically realized as well as the stark differences between these bosonic models and their fermionic counterparts.

1.2 Parametrically Driven Bosonic Systems

In fermionic superconductors, the pairing mechanism is the result of a mean-field analysis of a genuine two-body interaction. Taking this idea over to the bosonic case, we reason that one may also obtain a non-particle conserving Hamiltonian by using a non-linear Hamiltonian as the starting point. Fortunately, such non-linear interactions are commonplace in several areas of physics including optomechanics [5], circuit QED [6], and cavity QED [7] to name a few. To obtain the relevant physics, one must drive the system by pumping an auxiliary bosonic mode, i.e. with a laser (one obtains similar terms by considering a mean-field treatment of an interacting bosonic system when one has a condensate). Focusing on a single bosonic mode $\hat{a}$, after all approximations have been made the relevant Hamiltonian becomes [8] ($\hbar = 1$ here and throughout)

$$\hat{H}_{\text{SMS}} = \omega_0 \hat{a}^\dagger \hat{a} + i\Delta \left(e^{-i2\omega_P t} \hat{a}^\dagger \hat{a}^\dagger - e^{i2\omega_P t} \hat{a}\hat{a} \right) \tag{1.2.1}$$

where ω_0 the bare frequency of mode $\hat{a}$ and ω_P is the pump frequency. The precise form of Δ will vary depending on the physical implementation, but will always be proportional to the drive amplitude and will be referred to as such. We now make a rotating-frame transformation

$$\hat{H}_{RSMS} = \hat{U}^\dagger(t) \hat{H}_{SMS} U(t) - i\hat{U}^\dagger(t) \frac{d}{dt} \hat{U}(t) \tag{1.2.2}$$

$$\hat{U}(t) = e^{-i\omega_P \hat{a}^\dagger \hat{a} t} \tag{1.2.3}$$

In this rotating frame, the Hamiltonian is time independent

$$\hat{H}_{\text{RSMS}} = \omega \hat{a}^\dagger \hat{a} + i\Delta \left(\hat{a}^\dagger \hat{a}^\dagger - \hat{a}\hat{a} \right) \tag{1.2.4}$$

with $\omega = \omega_0 - \omega_P$. It is immediately evident that a fermionic equivalent of Eq. (1.2.4) would be trivial. Fermionic statistics would force the particle non-conserving term to be zero, since physically, a fermionic mode can't be doubly occupied. Of course, bosons have no such constraint on occupation number. This is our first insight that, even though we have no interactions, particle statistics play an important role in parametrically driven bosonic systems. This is perhaps most obvious by considering the dynamics generated by the Hamiltonian in Eq. (1.2.4). The Heisenberg equations of motion for $\hat{a}$ and $\hat{a}^\dagger$ are

$$i\partial_t \begin{pmatrix} \hat{a}(t) \\ \hat{a}^\dagger(t) \end{pmatrix} = \begin{pmatrix} \omega & 2i\Delta \\ 2i\Delta & -\omega \end{pmatrix} \begin{pmatrix} \hat{a}(t) \\ \hat{a}^\dagger(t) \end{pmatrix} \tag{1.2.5}$$

Thus, despite starting with a Hermitian Hamiltion $\hat{H}$, the dynamics are by a non-Hermitian matrix. We must be careful when analyzing the dynamics of the system since we can no longer immediately assume that the eigenvalues of the dynamical matrix are real. In fact, if we drive on resonance $\omega_P = \omega_0$, the eigenvalues of the dynamical matrix are simply $\pm 2i\Delta$. In this case, the equations of motion are trivial to solve and give

$$\hat{a}(t) = \cosh(2\Delta t)\hat{a} + \sinh(2\Delta t)\hat{a}^\dagger \tag{1.2.6}$$

The complex eigenvalues have resulted in exponential growth instead of the usual oscillatory terms whose frequencies are determined by the energies. Consequently, the number of photons in mode $\hat{a}$ will diverge as $t \to \infty$, even if our initial state is in the vacuum state. We must remember however that our dynamics were generated by a linearized mean-field version of a genuine non-linear Hamiltonian. As the photon number starts to diverge, the non-linear effects play an important role in the dynamics and, ultimately, make the system stable once again.

The driving term Δ has thus rendered the system parametrically unstable, a feature of driven bosonic systems which have no fermionic counterpart. After a moments thought, it is perhaps not surprising that we have a diverging photon number with this simple model: when driving on resonance, Eq. (1.2.4) tells us that our pump adds and remove pairs of photons with no energy cost. We can thus avoid the issue of parametric instability by, for example, driving off resonance or adding dissipation.

In this thesis we are interested in studying quadratic particle non-conserving bosonic Hamiltonians which, despite having essentially classical equations of motion, are still able to generate genuine quantum states. For example, let yet once again consider the Hamiltonian in Eq. (1.2.4) again focusing on the case where we drive on resonance. If we assume that we start in the vacuum state, then for all times $\langle \hat{x}(t) \rangle = \langle \hat{p}(t) \rangle = 0$. The variance of the quadrature degrees of freedom $\hat{x} = \frac{1}{\sqrt{2}}(\hat{a} + \hat{a}^\dagger)$ and $\hat{p} = \frac{1}{\sqrt{2}i}(\hat{a} - \hat{a}^\dagger)$

$$\langle \hat{x}^2(t) \rangle = \frac{1}{2} e^{4\Delta t} \qquad \langle \hat{p}^2(t) \rangle = \frac{1}{2} e^{-4\Delta t} \tag{1.2.7}$$

grows and decays exponentially in time, while still saturating Heisenberg's uncertainty. Such states are called squeezed states and their usefulness is immediately obvious: if one can couple a physical observable to the quadrature which gets squeezed, the uncertainty in the resulting measurement will be greatly reduced.

Non-particle conserving quadratic Hamiltonians can also be used to generate states which are entangled, a manifestly quantum effect. The simplest such example is a two-mode squeezing (TMS) Hamiltonian

$$\hat{H}_{TMS} = i\Delta \left(\hat{a}\hat{b} - \hat{a}^\dagger \hat{b}^\dagger \right). \tag{1.2.8}$$

with $\hat{a}$ and $\hat{b}$ two bosonic modes. Assuming that the initial state is the vacuum (and the resulting stated is called a two-mode squeezed vacuum state), we can write down the many-body wavefunction in the Fock basis of both modes $\hat{a}$ and $\hat{b}$ as [8]

$$e^{t\,\Delta\left(\hat{a}\hat{b}-\hat{a}^\dagger\hat{b}^\dagger\right)}\left|0\right\rangle = \frac{1}{\cosh(t\Delta)}\sum_{n=0}^{\infty}\tanh^n(t\Delta)\left|nn\right\rangle \tag{1.2.9}$$

After tracing out the $\hat{b}$ mode, we are left with the reduced density matrix for the $\hat{a}$ mode

$$\hat{\rho}_{\hat{a}} = \frac{1}{\cosh^2(t\Delta)}\sum_{n=0}^{\infty}\tanh^{2n}(t\Delta)\left|n\right\rangle\left\langle n\right| \tag{1.2.10}$$

which is a thermal state with effective Boltzmann factor $\tanh^2(t\Delta)$. Thus, even though we started with a pure state, we are left with a mixed state. We conclude that a two-mode squeezed vacuum state is indeed entangled. Furthermore, a larger squeezing parameter means the two modes are more strongly entangled. Indeed, in this limit the effective temperature of the reduced density matrix goes to infinity. One can in fact readily quantify the amount of entanglement of a two-mode squeezed state via the log-negativity [9].

1.3 Model

Having discussed how one can physically realize a bosonic analogue of a fermionic superconductor, as well as the corresponding novel dynamics that arise due to bosonic statistics, we are now in a position to study the bosonic version of the Kitaev chain. The simplest such model one could consider calling a bosonic Kiatev chain is by simply replace the fermionic operators in Eq. (1.1.1) with bosonic ones.

$$\hat{H}_B = \frac{1}{2}\sum_j\left(t\hat{a}^\dagger_{j+1}\hat{a}_j + i\Delta\hat{a}^\dagger_{j+1}\hat{a}^\dagger_j + h.c.\right) = \sum_k\left[t\cos k\,\hat{a}^\dagger_k\hat{a}_k + i\frac{\Delta}{2}\cos k\left(\hat{a}^\dagger_k\hat{a}^\dagger_{-k} - h.c.\right)\right], \tag{1.3.1}$$

where we've assumed periodic boundary conditions and Fourier transformed to momentum space. One can readily compute the energies $E_{\pm}(k) = \pm\sqrt{t^2 - \Delta^2}\cos k$ and conclude that stability is realized throughout the band if and only if $t > \Delta$. Furthermore, the eigenstates of this model are plane waves, a consequence of translational invariance.

Like in the fermionic Kitaev chain, we now ask how the presence of boundaries affects both the energies and eigenstates of the Hamiltonian Eq. (1.3.1). The intuition obtained from the fermionic case tells us that the finite sized version of this model should be trivial seeing as the vector $\mathbf{h}_B(k)$ in Eq. (1.3.1) no longer winds around the origin. This intuition turns out to be correct: while momentum is no longer conserved due to the presence of boundaries, we may simply form standing waves of momentum k and $-k$ to diagonalize the Hamiltonian. More specifically, focusing on a finite sized system of N lattice sites, we have

$$\begin{aligned} \hat{H}_B &= \frac{1}{2}\sum_{j=1}^{N-1}\left(t\hat{a}_{j+1}^\dagger \hat{a}_j + i\Delta \hat{a}_{j+1}^\dagger \hat{a}_j^\dagger + h.c.\right) \\ &= \sum_{n=1}^{N}\left[t\cos k_n\, \hat{a}_{k_n}^\dagger \hat{a}_{k_n} + i\frac{\Delta}{2}\cos k_n \left(\hat{a}_{k_n}^\dagger \hat{a}_{k_n}^\dagger - h.c.\right)\right], \end{aligned} \tag{1.3.2}$$

with $\hat{a}_{k_n}$ a standing wave annihilation operator

$$\hat{a}_{k_n} = \sqrt{\frac{2}{N+1}}\sum_{j=1}^{N}\sin(k_n j)\hat{a}_j, \tag{1.3.3}$$

and $k_n = n\pi/(N+1)$. The finite chain with open boundary conditions is essentially no different from the infinite lattice or the chain with periodic boundary conditions. One readily sees that stability is achieved throughout the band if and only if $t > \Delta$, just like in the system without boundaries. Furthermore, the eigenstates of the finite sized system are standing waves and thus do no exhibit any localization.

To obtain any interesting physics, we must break inversion symmetry (i.e. the operation which sends j to $-j$). If we did not, then the Hamiltonian would always be diagonal in the standing wave basis introduced above. The easiest route to breaking inversion symmetry is by making the hopping amplitude purely imaginary $t \to it$. Again assuming we have a finite lattice of N sites, we have

$$\hat{H}_B \equiv \frac{1}{2} \sum_{j=1}^{N-1} \left(it \hat{a}_{j+1}^{\dagger} \hat{a}_j + i\Delta \hat{a}_{j+1}^{\dagger} \hat{a}_j^{\dagger} + h.c. \right) \tag{1.3.4}$$

Note that phase factor in the hopping can't be simply gauged away, as would be the case if $\Delta = 0$. Although the standing wave basis no longer diagonalizes the Hamiltonian, it is not obvious that this new model is any more interesting than the one without any phases.

Taking inspiration from the fermionic model, we now express Eq. (1.3.4) in a new basis of localized Hermitian operators $\hat{a}_j = \frac{1}{\sqrt{2}}(\hat{x}_j + i\hat{p}_j)$, i.e. the canonical quadrature operators. A direct substitution yields

$$\hat{H}_B \equiv \frac{1}{2} \sum_{j=1}^{N} \left(-(t-\Delta)\hat{x}_{j+1}\hat{p}_j + (t+\Delta)\hat{p}_{j+1}\hat{x}_j \right) \tag{1.3.5}$$

The structure here is analogous to the fermionic case: $\hat{x}$ quadratures are only coupled to $\hat{p}$ quadratures, and further, there is an asymmetry in the coupling between $\hat{x}_j$ and $\hat{p}_{j\pm1}$ (c.f. Eq. (1.1.7)).

In this thesis we study the bosonic Kitaev chain as introduced above. In Chapter (2) we examine the dynamics of our model and demonstrate that propagation is heavily quadrature dependent and uniquely bosonic in nature. Chapter (3) explores the effect of boundaries; we find that it drastically affects both the dynamics and eigenstates of our system. We then discuss in Capter (4)the possibility of using a generalized version of our model to generate useful Gaussian entangled states. Finally, Chapter (5) gives a brief summary and possible directions for future work.

2

Phase-Dependant Transport

The fermionic Kitaev chain is gapped: the hopping asymmetry leads to isolated Majorana modes on the edges while the bulk can only carry supercurrent. As we have seen in the previous chapter, the bosonic Kitaev chain has a similar asymmetric hopping strucutre in the basis of quadrature operators. In this section, we study the dynamics of our model and show that they depend heavily on the global phase of the photonic excitation. Further the transport properties are uniquely bosonic, having no fermionic counterpart.

2.1 Quadrature Representation

Perhaps the most dramatic consequence of the pairing structure in Eq. (1.3.5) lies in the dynamics. The Heisenberg equations of motion corresponding to $\hat{H}_B$ are

$$\dot{\hat{x}}_j = \frac{t+\Delta}{2}\hat{x}_{j-1} - \frac{t-\Delta}{2}\hat{x}_{j+1} \tag{2.1.1}$$

$$\dot{\hat{p}}_j = \frac{t-\Delta}{2}\hat{p}_{j-1} - \frac{t+\Delta}{2}\hat{p}_{j+1}. \tag{2.1.2}$$

Note that the dynamics of the $\hat{x}$ quadratures are completely decoupled from that of the $\hat{p}$ quadratures. Furthermore, each quadrature is forced in an asymmetric manner by its neighbors. As $\Delta \to t$, we have completely asymmetry: $\hat{x}$ quadratures are only forced by their neighbor to the left, $\hat{p}$ by their neighbors to the right. If we imagine quadratures are particles, we would thus expect chiral propagation: x "particles" would only propagate to the right, p particles to the left. As we shall soon see, this picture is essentially correct: Eqs. (2.1.1)-(2.1.2) imply that the propagation dynamics of a photonic wavepacket is determined by it's global *phase*.

Before proceeding, we must recall the discussion in the previous chapter and ask the question: is $\hat{H}_B$ stable? Focusing at the moment on our finite chain, we find that the system is stable as long as $t > \Delta$, independent of the chain length. In this regime, the parametrically driven system is unitarily equivalent to a simple particle conserving tight-binding model, as we now show.

We first define the parameter r via

$$e^{2r} = \frac{t+\Delta}{t-\Delta}, \tag{2.1.3}$$

which is a measure of the asymmetry in the left-right quadrature coupling. We can then define a local position-dependent unitary transformation by

$$\hat{U}\hat{x}_j\hat{U}^\dagger = e^{r(j-j_0)}\hat{\tilde{x}}_j, \qquad \hat{U}\hat{p}_j\hat{U}^\dagger = e^{-r(j-j_0)}\hat{\tilde{p}}_j. \tag{2.1.4}$$

Here, $\hat{\tilde{x}}$ and $\hat{\tilde{p}}$ are new canonical quadrature degrees of freedom and j_0 is an arbitrary real number. In this new basis, we find

$$\begin{aligned}
\hat{U}\hat{H}_B\hat{U}^\dagger &= \frac{\tilde{t}}{2}\sum_j \left(-\hat{\tilde{x}}_{j+1}\hat{\tilde{p}}_j + \hat{\tilde{p}}_{j+1}\hat{\tilde{x}}_j\right) \\
&= \frac{1}{2}\sum_j \left(i\tilde{t}\hat{\tilde{a}}^\dagger_{j+1}\hat{\tilde{a}}_j + h.c.\right),
\end{aligned} \tag{2.1.5}$$

with

$$\tilde{t} = \sqrt{t^2 - \Delta^2} = t/\cosh(r). \tag{2.1.6}$$

Thus, in the regime $t > \Delta$, $\hat{H}_B$ is unitarily equivalent to a simple, particle-conserving Hamiltonian with a renormalized hopping amplitude $\tilde{t}$. Note that the transformed Hamiltonian is completely independent of j_0, a consequence of $\hat{H}_B$ being invariant under any spatially constant squeezing transformation which doesn't mix $\hat{x}$ and $\hat{p}$ quadratures, i.e. $\hat{x}_j \to e^z\hat{x}_j$, $\hat{p}_j \to e^{-z}\hat{p}_j$.

We also briefly comment on the special case $t = \Delta$. In this case, Eq. (1.3.5) implies that the coupling is completely asymmetric such that $\hat{x}_j$ only couples to $\hat{p}_{j+1}$ and not $\hat{p}_{j-1}$. In a finite chain of N sites, there are two quadratures $\hat{x}_1$ and $\hat{p}_N$ which drop out of the Hamiltonian. While in the fermionic model, these two decoupled edge modes are of great interest, this is not the case here. Unlike Majoranas, one can't form a new bosonic degree of freedom from two spatially separated quadratures. More explicitly, since $[\hat{x}_1, \hat{p}_N] = 0$, no operator $\hat{f}$ which is a linear combination of these two quadratures can possibly satisfy the bosonic commutations relation $[\hat{f}, \hat{f}^\dagger] = \hat{1}$. Although these decoupled quadratures are quantum non-demolition variables (QND), meaning that their conjugate variables have no dynamics, their existence requires precisely tuning to the threshold of instability. We will thus focus on the regime $t > \Delta$ throughout this thesis.

2.2 Phase-sensitive chiral transport

Eqs. (2.1.1)-(2.1.2) imply that photonic excitations propagate in a manner that is directly determined by their phase. To characterize the chiral nature of the transport, we compute the quadrature-quadrature Green's functions. This can be readily computed by using the position dependent squeezing transformation Eq. (2.1.4). The only non-zero Green's functions are

$$\begin{aligned} G_x^R[j,j';\omega] &\equiv -i\int_0^\infty dt\, e^{i\omega t}\langle[\hat{x}_j(t),\hat{p}_{j'}(0)]\rangle \\ &= i\tilde{G}_0^R[j,j';\omega]e^{r(j-j')} \end{aligned} \tag{2.2.1}$$

$$G_p^R[j,j';\omega] = -i\tilde{G}_0^R[j,j';\omega]e^{-r(j-j')} \tag{2.2.2}$$

Here, $\tilde{G}_0^R[j,j';\omega]$ is the retarded Green's function of a simple, particle conserving tight-binding chain with hopping matrix element $i\tilde{t}$.

The Green's function $G_x^R[j,j';\omega]$ describes propagation of the x quadrature within the lattice; in particular it describes how $\hat{x}_j$ responds to a perturbation which directly forces $\hat{x}_{j'}$. We note that since x and p quadratures are dynamically decoupled, forcing $\hat{x}_{j'}$ never induces a response in $\hat{p}_j$. The structure of the Green's function makes the expected chirality evident: x quadratures propagate and are amplified(de-amplified) as they propagate to the right (left) and vice-versa for the p quadratures. Note that the local Green's function ($j = j'$) are independent of the squeezing parameter r and are in fact equal to that of a particle conserving tight-binding model.

Remarkably, the above structure still holds if we introduce position dependent loss. We assume this loss is Markovian and model it using standard input-output theory [10, 11]. The loss rate κ_j on each site could be due to coupling to the waveguides or to internal loss. The Heisenberg-Langevin equations for the local quadratures $\hat{x}_j$ and $\hat{p}_j$ reads

$$\dot{\hat{x}}_j = \frac{\tilde{t}}{2}\left(e^{r}\hat{x}_{j-1} - e^{-r}\hat{x}_{j+1}\right) - \frac{1}{2}\kappa_j\hat{x}_j - \sqrt{\kappa_j}\hat{x}_j^{(\text{in})}, \tag{2.2.3}$$

$$\dot{\hat{p}}_j = \frac{\tilde{t}}{2}\left(e^{-r}\hat{p}_{j-1} - e^{r}\hat{p}_{j+1}\right) - \frac{1}{2}\kappa_j\hat{p}_j - \sqrt{\kappa_j}\hat{p}_j^{(\text{in})}. \tag{2.2.4}$$

$\hat{x}_j^{(\text{in})}$ and $\hat{p}_j^{(\text{in})}$ are the quadratures of the input fields impinging on loss port j. It could, for example, corresponds to a classical drive field or vacuum noise.

Although we have broken translational invariance by introducing site dependent loss, we are still able to map the system to a particle conserving model. One simply performs the same squeezing transformation defined in Eq. (2.1.4) on *both* the cavity modes and input fields. Although the input modes are now squeezed in this frame, the linearity of the equations of motion imply that the Green's function remain unchanged. Thus, the Green's function of the system with loss will still have the form of Eqs.(2.2.1)-(2.2.2) with $\tilde{G}_0^R[j, j'; \omega]$ the photonic Green's function of a tight-binding model with hopping amplitude $i\tilde{t}$ and on-site loss κ_j.

2.3 Scattering Properties

We now consider the case where input-output waveguides are attached to our lattice, and ask how signals injected into these waveguides are scattered. Since our equations of motion are linear, the scattering matrix completely characterizes such transport properties. Input-output theory gives us a simple relation between the input, output and cavity modes via the boundary conditions $\hat{a}_j^{(\text{out})} = \hat{a}_j^{(\text{in})} + \sqrt{\kappa_j}\hat{a}_j$ and Heisenberg-Langevin equations in Eqs. (2.2.3),(2.2.4) [11]. Since x and p quadratures are dynamically decoupled in our system, the scattering matrix takes a particularly simple form in this basis

$$\hat{x}_j^{(\text{out})}[\omega] = \sum_{j'} s^x_{jj'}[\omega]\hat{x}_{j'}^{(\text{in})}[\omega], \qquad \hat{p}_j^{(\text{out})}[\omega] = \sum_{j'} s^p_{jj'}[\omega]\,\hat{p}_{j'}^{(\text{in})}[\omega] \tag{2.3.1}$$

The scattering matrices are completely determined by the Green's function of the cavity system, and thus inherits their unique structure

$$s^x_{jj'}[\omega] = e^{r(j-j')}\tilde{s}_{jj'}[\omega], \tag{2.3.2}$$

$$s^p_{jj'}[\omega] = e^{-r(j-j')}\tilde{s}_{jj'}[\omega]. \tag{2.3.3}$$

where $\tilde{s}_{jj'}[\omega]$ is the scattering matrix of a particle conserving tight-binding model with on-site loss κ_j and hopping matrix element $i\tilde{t}$. The scattering matrix in such a system is phase-independent, and is thus the same for both quadratures. As expected, scattering in our full system can be understood by examining the dynamics of the unperturbed system: $\hat{x}$ quadrature signals are amplified (de-amplified) when transmitted from left to right (right to left) while $\hat{p}$ quadratures exhibit the opposite behavior (see Fig. 2.1).

Our system thus represents a unique kind of phase-sensitive amplifier. These devices amplify one quadrature (while de-amplifying the other) without the needed for added noise. They are also used as a resource, producing non-classical squeezed states. Conventional amplifiers amplify only in one direction, due to phase matching, or amplify the same quadrature regardless of transmission direction. In contrast, here we obtain amplification in both directions, but in different orthogonal quadratures. Note also that the end to end transmission gain $|s^x_{1N}[\omega]|^2 = |s^p_{N1}p[\omega]|^2$ scales like e^{2rN}, whereas the amplification bandwidth goes like $\tilde{t} = t/\cosh(r)$. Thus, if we have a long chain and a small parameter r, we can get arbitrarily large gain without greatly reducing the bandwidth. We have therefore sidestepped the usual gain-bandwidth product restriction that

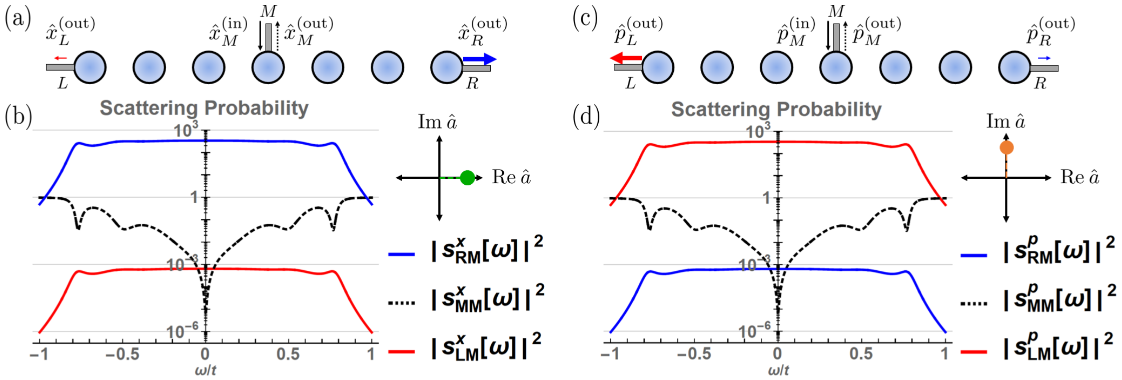

Figure 2.1: Scattering properties of the bosonic Kitaev-Majorana chain: (a) Schematic of the setup. The leftmost, middle and rightmost sites are attached to waveguides (coupling rates κ_L, κ_M and κ_R respectively). A signal with a frequency ω and global phase $\theta = 0$, corresponding to an x excitation, is injected in the middle waveguide and is amplified (deamplified) as it propagates to the right (left). (b) Amplitude squared of the scattering matrix elements plotted as a function of frequency of the input signal. As expected, signals propagating to the right (left) and amplified (deamplified). Note the reflection probability (black) is bounded by unity. (c) Same setup as in (a), except the phase of the signal is now $\theta = \frac{\pi}{2}$, corresponding to a p excitation. (d) The signal is now amplified (deamplified) as it propagates to the left (right). For (b),(d), we take $N = 13$ sites, $\Delta = t/2$, uniform on-site internal loss rate $\kappa = 10^{-2}t$, and waveguide couplings $\kappa_M = 2\kappa_L = 2\kappa_R = 2t$.

most amplifiers adhere to.

Viewed as an amplifier, the bosonic Kitaev chain has another unique property: while we have a large amount of transmission gain, there is never any reflection gain. This follows direction from Eqs. (2.3.2)-(2.3.3), which tells us that $s^x_{jj}[\omega] = s^p_{jj}[\omega] = \tilde{s}_{jj}[\omega]$. Reflection in our system is phase insensitive and equal to that of a particle conserving tight-binding model and thus is bounded by unity. The lack of reflection gain is useful in many settings where one would like to protect the fragile signal impinging on the input port.

The lack of reflection gain can be intuitively understood by returning to the equations of motion Eqs. (2.1.1)-(2.1.2). Due to the open boundaries and nature of the hopping, reflection requires an equal amount of left-to-right and right-to-left propagation. The chiral nature of amplification then implies that the net amplification for such a process will always be zero: amplification in one direction is perfectly canceled by de-amplification in the opposite direction.

3

Sensitivity to Edges and Disorder

As we have already seen, a remarkable feature of the Kitaev chain is its striking sensitivity to boundary conditions. In an infinite or periodic system there is an energy gap centered around zero and corresponding plane-wave eigenfunctions, yet for open boundary conditions there are zero energy Majorana modes localized on the edges. We find that our bosonic Kitaev chain exhibits an even stronger sensitivity to boundary conditions: the periodic system is characterized by dynamically unstable delocalized modes, whereas the presence of boundaries renders all modes stable and localized on the edges. We explain further in what follows.

3.1 Spectrum

Let us first consider our bosonic Kitaev chain with periodic boundary conditions. The presence of the phase in the hopping parameter $t \to it$ changes the single particle-conserving dispersion $t\cos(k) \to t\sin(k)$ (see Eq.(1.3.1)) such that the Hamiltonian now reads

$$\hat{H}_B = \frac{1}{2}\sum_k \left(t\sin k(\hat{a}_k^\dagger \hat{a}_k - \hat{a}_{-k}^\dagger \hat{a}_{-k}) + i\Delta\cos k \left(\hat{a}_k^\dagger \hat{a}_{-k}^\dagger - h.c.\right)\right) \tag{3.1.1}$$

We can already conclude that the system is unstable for an arbitrarily strong driving strength Δ. The presence of the phase has made the detuning between modes k and $-k$ zero, such that the pairing term with amplitude $\Delta\cos k$ is resonant. Indeed, one can readily compute the complex energies $E_{k,\pm} = t\sin k \pm i\Delta\cos k$. Furthermore, due to translational invariance, the eigenstates are simply plane-wave states.

Despite being intuitively reasonable, the behavior of the periodic boundary condition system is completely different than the corresponding system with open boundary conditions. The former, as demonstrated in Eq.(2.1.5), can be mapped onto a particle conserving tight-binding model with hopping amplitude $i\tilde{t} = \sqrt{t^2 - \Delta^2}$. Consequently, for any $\Delta < t$, there is no instability: its spectrum is entirely real and given $E_n = \tilde{t}\cos k_n$ with $k_n = n\pi/(N+1)$. We thus have a dramatically different spectrum depending on the choice of boundary conditions, as demonstrated in Fig. (3.1). Note that this conclusion is independent of system size.

For an intuitive understanding as to why the different boundary conditions give rise to such different dynamics, we return to our discussion of the reflection gain. In an open boundary setup, reflection requires an equal amount of right-to-left and left-to-right propagation. The lack of reflection gain is a consequence of a delicate balance between amplification in one direction and deamplification in the opposite direction. A photonic wavepacket which undergoes a single round trip within the open boundary system will not be amplified, which precludes instability. With periodic boundary conditions in place however, this intuitive picture no longer holds. In this ring geometry, a wavepacket with a definite global phase corresponding to e.g. an x excitation propagating clockwise will

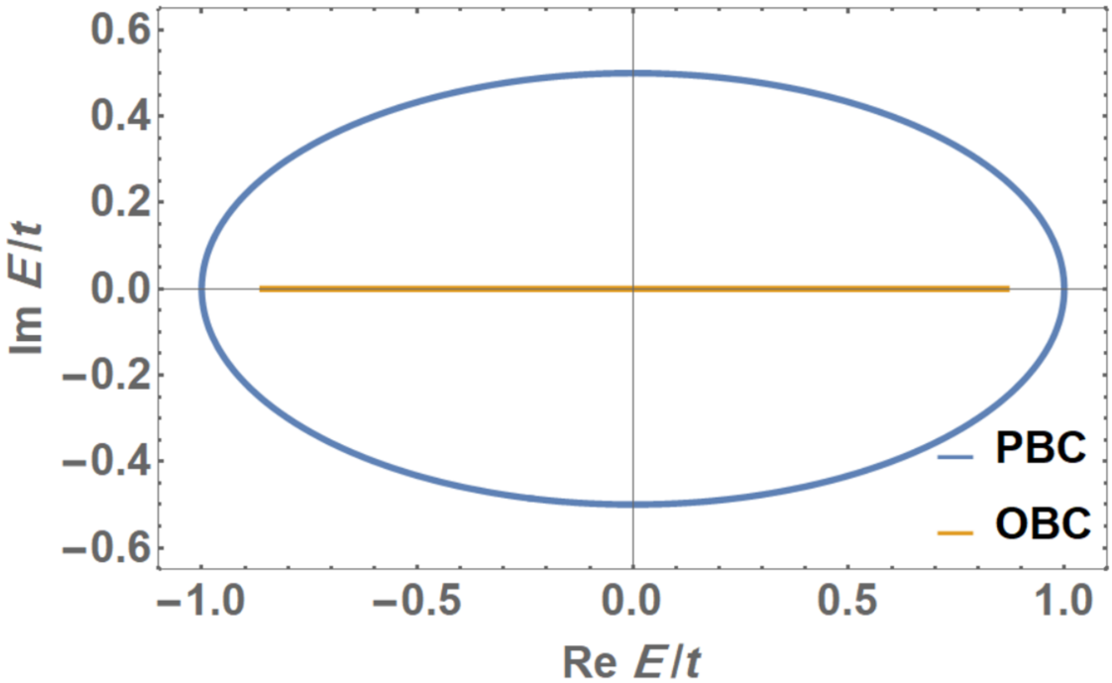

Figure 3.1: Spectrum of the system with periodic boundary condition (PBC) $E^{PBC}_{k,\pm} = t\sin(k) \pm i\Delta\cos(k)$ versus open boundary conditions (OBC) $E^{OBC}_{k} = \sqrt{t^2-\Delta^2}\cos(k)$ with $\Delta = t/2$. The spectrum with PBC is complex for any non-zero Δ, indicating parametric instability. In contrast, the system with OBC is stable as long as $t > \Delta$, regardless of system size.

be amplified by a factor of e^{rN} after a single round trip. The subsequent infinite number of round trips in the chain lead to a diverging excitation amplitude; the system is now unstable for arbitrary Δ (see. Fig. 3.1).

3.2 Eigenstates

As we have just seen, the spectrum of the bosonic Kitaev chain is extremely sensitive to the boundary conditions under consideration. It is perhaps then not surprising that the eigenstates of the finite open chain bear no resemblance to those of the infinite sized system. Naively the eigenstates of the finite sized system are linear combinations of plane-wave states whose momenta have the same bulk energy. Yet our local squeezing transformation Eq. (2.1.4) already indicates that this intuition must fail. After the squeezing transformation, the Hamiltonian is readily diagonalized $\hat{H}_B^{OBC} = \sum_n E_n \beta_n^\dagger \beta_n$ where β_n are Bogoliubov modes of the original photonic operators

$$\beta_n = \sum_{j=1}^{N} \left(u_n(j)\hat{a}_j - v_n(j)\hat{a}_j^\dagger \right). \tag{3.2.1}$$

Here, $u_n(j)$ and $v_n(j)$ are the "particle" and "anti-particle" wavefunctions respectively

$$u_n(j) = \sqrt{\frac{2}{N+1}} i^{-j} \sin(k_n j) \cosh(r(j - j_0)) \tag{3.2.2}$$

$$v_n(j) = \sqrt{\frac{2}{N+1}} i^{-j} \sin(k_n j) \sinh(r(j - j_0)). \tag{3.2.3}$$

where the squeeze parameter r is defined in Eq. (2.1.3). Note that there are many different ways to diagonalize the Hamiltonian through the free parameter j_0, which corresponds the origin of our squeezing transformation.

Both the particle and antiparticle part of the wavefunctions are localized; they both have an exponential dependence on position and their weight is concentrated at the edges. On the other hand, for a given eigenmode, the contribution from each site to the symplectic norm $|u_n(j)|^2 - |v_n(j)|^2$ does not exhibit any localization. This quantity is in fact completely independent of the two photon driving term Δ, consistent with the local Green's function being phase insensitive and independent of r. Consequently, is it difficult to measure the localization in our system with a purely local probe; one must consider a non-local probe such as transmission.

3.3 Disorder Effects

We now explore, both qualitatively and quantitatively, how the bosonic Kitaev chain is affected by the presence of disorder. We focus exclusively on a finite chain of N sites with open boundary conditions. The simplest kind of disorder we could imagine is random on-site losses κ_j. Yet we've already seen that this disorder is fairly unimportant; we can still map our system onto a particle conserving model via a local squeezing transformation, where the accompanying fluctuations describe squeezed noise (see Eqs. (2.2.3)-(2.2.4)). Thus, our system is unitarily equivalent to a tight-binding model with disordered on-site loss. Despite breaking translational invariance, causing reflections within the system, we still remain stable in this case.

The situation is very different if we have a non-zero on-site energies described by

$$\hat{H}_{\rm dis} = \sum_{j=1}^{N} \omega_j \hat{a}_j^\dagger \hat{a}_j. \tag{3.3.1}$$

Our foremost concern is that the presence of varying on-site energies can cause instability even in the clean chain condition $\Delta < t$. This can be understood by moving to our squeezed basis defined by Eq. (2.1.4). While the loss terms are invariant under this squeezing, the on-site potential terms in this frame do not conserve particle number

$$\hat{U}\hat{H}_{\rm dis}\hat{U}^\dagger = \sum_{j=1}^{N} \omega_j \Big(\cosh(2r(j-j_0))\hat{\hat{a}}_j^\dagger \hat{\hat{a}}_j + \frac{1}{2}\sinh(2r(j-j_0)) \left[\hat{\hat{a}}_j^\dagger \hat{\hat{a}}_j^\dagger + \hat{\hat{a}}_j \hat{\hat{a}}_j \right] \Big) \tag{3.3.2}$$

where we've thrown away terms proportional to the identity. Thus, it is generically impossible to move to a frame where particle number is conserved and we can no longer preclude dynamical instability. In the special case where there is only one impurity at site $j = j_{\mathrm{imp}}$, there is never instability; we may set the origin of the squeezing to be the site of the impurity $j_0 = j_{\mathrm{imp}}$ thereby mapping our system yet again onto a particle conserving model. This is no longer possible if there is even a single additional impurity located at another site.

We now seek a more physical understanding as to how on-site potential disorder causes instability. To this end, let us return to our trusty equations of motion in the quadrature basis which now reads

$$\dot{\hat{x}}_j = \frac{\tilde{t}}{2}\left(e^{r}\hat{x}_{j-1} - e^{-r}\hat{x}_{j+1}\right) - \frac{1}{2}\kappa_j \hat{x}_j + \omega_j \hat{p}_j, \tag{3.3.3}$$

$$\dot{\hat{p}}_j = \frac{\tilde{t}}{2}\left(e^{-r}\hat{p}_{j-1} - e^{r}\hat{p}_{j+1}\right) - \frac{1}{2}\kappa_j \hat{p}_j - \omega_j \hat{x}_j. \tag{3.3.4}$$

We see that the main effect of this potential disorder is to dynamically couple the x and p quadratures. Scattering off of these impurities can then change the *phase* of the photonic wavepacket (i.e. covert an x excitation to p excitation and vice-versa). The chiral nature of the amplification then implies that multiple reflections between several impurities can lead to indefinite amplification and thus instability. This is in contrast to scattering off of on-site loss or boundaries, processes which manifestly preserve the phase of excitation and hence do not lead to any instability.

We now wish to qualitatively assess the impact of on-site potential disorder. To do so, we perform a numerical disorder average. We take the ω_j in Eq. (3.3.1) to be random independent variables, uniformly drawn from the interval $[-W, W]$, with W being the disorder strength. If there is a significant amount of amplification, we expect frequency disorder to be highly detrimental to stability; the multiple phase-changing reflections become more relevant and can lead to indefinite amplification. On the other hand if $W \ll \tilde{t}$ and r, N not too large, we expect disorder effects to be largely mitigated. The validity of our claim is confirmed by computing the disorder averaged

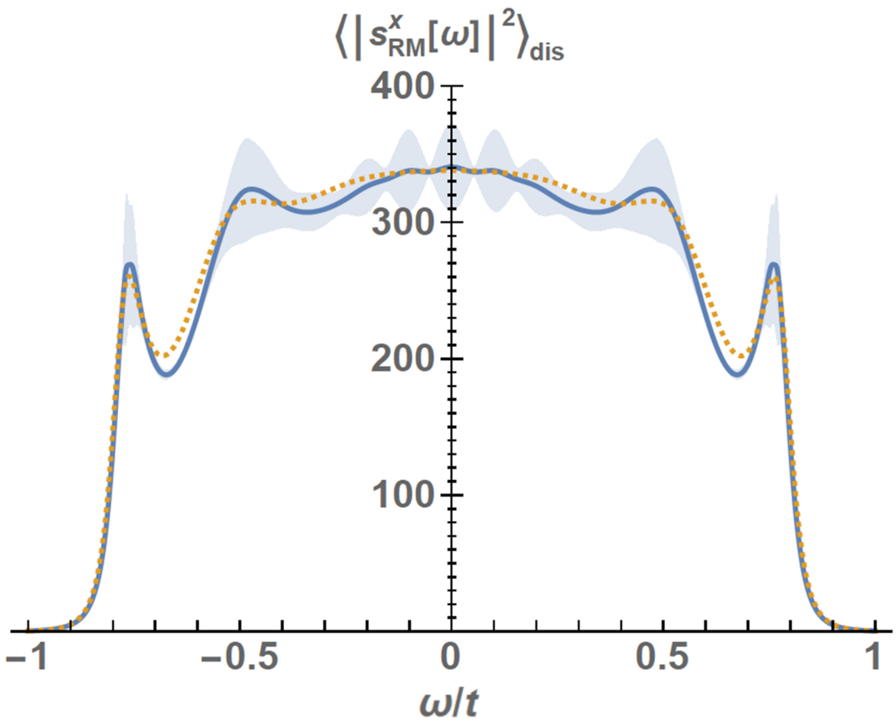

Figure 3.2: Disorder averaged transmission coefficient $\langle |s^x_{\mathrm{RM}}[\omega]|^2 \rangle_{\mathrm{dis}}$ for the same setup as is Fig. 2.1, but with on-site disorder (disorder strength $W = 10^{-3}t$). The shaded region corresponds to the variance and the dashed orange line corresponds to the clean system. Although stability is no longer guaranteed after introducing the disorder potential, with the chosen parameters, instability only occurs in less than 0.01% of realizations. For smaller values of r and/or N, one can tolerate even larger amounts of disorder. Parameters: $N = 13$ sites, $\Delta = t/2$, uniform on-site internal loss $\kappa = 10^{-2}t$, waveguide coupling rates $\kappa_M = 2\kappa_L = 2\kappa_R = 2t$.

scattering probabilities (10^4 realizations) in Fig. 3.2. There, for a similar setup as in Fig. 2.1 ($N = 13, r \approx 0.55$) but with disorder strength $W = 10^{-3}t$, less than 0.01% of realizations are unstable. The remaining realizations closely resembles the scattering of the clean system.

3.4 Non-Hermitian Topology

It is only natural to ask whether the striking properties of the bosonic Kitaev can be given a topological underpinning since, after all, the fermionic version is the prototypical example of a topological superconductor. As we've previously noted however, the fermionic and bosonic problems are not identical due to particle statistics; the dynamical matrix in the latter case is non-Hermitian. Consequently, the topology of parametrically driven bosonic systems is quite different than the fermionic version and has in fact been the subject of several recent studies [12–16]. In these papers however, one first assumes the driven system is stable, and only then proceed to examine its topology. For the bosonic Kitaev chain, this is clearly inadequate; with periodic boundary conditions any small pairing amplitude Δ leads to instability throughout the band. We therefore need a non-zero topological invariant which can be applied to unstable driven systems.

Attempting a full characterization parametrically unstable driven systems is far beyond the scope of this thesis. We will instead analyze a generalized bosonic Kitaev model on a semi-infinite lattice, and demonstrate that one can associate to it a non-zero topological number which guarantees the presence of edge modes. The model under consideration is described by the Hamiltonian

$$\hat{H}_{SI} = \frac{1}{2}\sum_{j=1}^{\infty}\left(te^{i\phi}\hat{a}^{\dagger}_{j+1}\hat{a}_j + \Delta e^{i\theta}\hat{a}^{\dagger}_{j+1}\hat{a}^{\dagger}_j + \nu\hat{a}^{\dagger}_j\hat{a}^{\dagger}_j + \omega_0\hat{a}^{\dagger}_j\hat{a}_j + h.c.\right). \tag{3.4.1}$$

where as before, t is the hopping matrix amplitude, and Δ is the nearest neighbor pairing amplitude with arbitrary hopping phase ϕ and θ respectively. We've also no longer assumed that we are driving on resonance (so that $\omega_0 \neq 0$) and furthermore we've introduced an on-site pairing term ν which we take to be real. To find an eigenstate α

with energy E, we make an ansatz of the form

$$\alpha = \sum_{j=1}^{\infty} \left(u_j \hat{a}_j - v_j \hat{a}_j^{\dagger} \right). \tag{3.4.2}$$

Heisenberg's equations of motion then turns into a set of coupled difference equations

$$A \begin{pmatrix} u_{j-1} \\ v_{j-1} \end{pmatrix} + (B - E\check{1}) \begin{pmatrix} u_j \\ v_j \end{pmatrix} + C \begin{pmatrix} u_{j+1} \\ v_{j+1} \end{pmatrix} = \begin{pmatrix} 0 \\ 0 \end{pmatrix} \tag{3.4.3}$$

where A, B and C are the 2×2 matrices

$$A = \frac{1}{2} \begin{pmatrix} te^{-i\phi} & \Delta e^{-i\theta} \\ -\Delta e^{i\theta} & -te^{i\phi} \end{pmatrix} \qquad B = \begin{pmatrix} \omega_0 & \nu \\ -\nu & -\omega_0 \end{pmatrix} \qquad C = \frac{1}{2} \begin{pmatrix} te^{i\phi} & \Delta e^{-i\theta} \\ -\Delta e^{i\theta} & -te^{-i\phi}. \end{pmatrix} \tag{3.4.4}$$

with boundary condition $u_0 = v_0 = 0$ since we have a semi-infinite chain.

Eq. (3.4.3) suggest that the wavefunctions should satisfy a sort of Bloch's theorem, i.e. we should try an ansatz of form

$$\begin{pmatrix} u_j \\ v_j \end{pmatrix} = z^j \begin{pmatrix} u \\ v \end{pmatrix}. \tag{3.4.5}$$

with z a complex number and the vector $(u, v)^T$ at this point is undetermined. Inserting the ansatz in Eq. (3.4.3) gives

$$\left(H(z) - E\check{1} \right) \begin{pmatrix} u \\ v \end{pmatrix} = \begin{pmatrix} 0 \\ 0 \end{pmatrix} \tag{3.4.6}$$

$$H(z) \equiv \left(z^{-1} A + B + zC \right). \tag{3.4.7}$$

We have introduced the matrix $H(z)$ because when z is on the unit circle, it is precisely this 2×2 dynamical matrix one must diagonalize to determine the band structure of the system with boundary conditions. Thus, when $|z| = 1$, we will refer to $H(z)$ as the bulk Hamiltonian.

For a non-trivial solution to Eq. (3.4.6), we must find the roots z_m of the polynomial $\det\big(H(z) - E\check{1}\big)$ and then subsequently require that $(u, v)^T$ is in the kernel of $H(z_m) - E\check{1}$. By the fundamental theorem of algebra, we can readily see that there will in general be four such roots z_m and corresponding vectors $(u^{(m)}, v^{(m)})^T$. We assume for simplicity that there are no repeating roots. The general form of the wavefunction at site j is then simply

$$\begin{pmatrix} u_j \\ v_j \end{pmatrix} = \sum_{m=1}^{4} c_m z_m^j \begin{pmatrix} u^{(m)} \\ v^{(m)} \end{pmatrix} \tag{3.4.8}$$

with c_m coefficients chosen to satisfy boundary conditions. In the present context we have two boundary conditions. First, we seek edge states whose wavefunctions vanish at infinity. The second boundary conditions is simply $u_0 = v_0 = 0$, by virtue of the semi-infinite nature of our system. The first boundary condition is easy to satisfy; if the root z_m lies outside the unit circle, hence it's norm is larger than unity, we set $c_m = 0$. The second boundary condition, in terms of the undetermined coefficients c_m is

$$\begin{pmatrix} u_0 \\ v_0 \end{pmatrix} = \sum_{m=1}^{4} c_m \begin{pmatrix} u^{(m)} \\ v^{(m)} \end{pmatrix} = \begin{pmatrix} 0 \\ 0 \end{pmatrix} \tag{3.4.9}$$

Generically speaking, for a non-trivial solution we need at least three of the c_m to be free parameters. Combining these two boundary conditions together, we thus arrive at the sufficient (but in general not necessary) condition which dictates when we have an edge state: *three roots of the polynomial* $\det\left(H(z) - E\check{1}\right)$ *must lie inside the unit circle*.

To characterize the number of roots which lie inside the unit circle, we simply use the argument principle, familiar from any introductory complex analysis class. Namely, we have

$$\frac{1}{2\pi i}\oint_{|z|=1} dz\partial_z \log\left(\det(H(z) - E\check{1})\right) = Z - P \tag{3.4.10}$$

where Z is the number of zeroes and P is the number of poles inside the contour, which in our case is the unit circle. Since $\det(H(z) - E\check{1})$ has a second order pole at $z = 0$ we conclude that if Eq. (3.4.10) is equal to one, we have an edge state. We can make this formula more visually appealing, and perhaps more intuitive, by factoring the determinant as $\det(H(z) - E\check{1}) = (E_+(z) - E)(E_-(z) - E)$ with $E_\pm(z)$ the bulk dispersions generalized to a complex parameter. The left hand side of Eq. (3.4.10) then reads

$$\frac{1}{2\pi i}\oint_{|z|=1} dz\partial_z \log\left(E_+(k) - E\right) + \frac{1}{2\pi i}\oint_{|z|=1} dz\partial_z \log\left(E_-(k) - E\right). \tag{3.4.11}$$

Eq. (3.4.11) is simply the sum of two winding numbers. It counts the number of time that the bulk dispersions $E_\pm(k)$ encircles the base point E in the complex plane. Thus, if the energy E lies "inside" the curve drawn out by the by the bulk dispersion in the complex plane, the corresponding eigenstate will be an edge mode. Needless to say, this quantity is manifestly an integer, and is invariant under small perturbation of system parameters. One may then argue that this quantity is a topological invariant. We point out that a number of similar looking formulas have been found recently in several papers [17, 18].

Although the previous analysis was done on a system which is infinite in one direction,

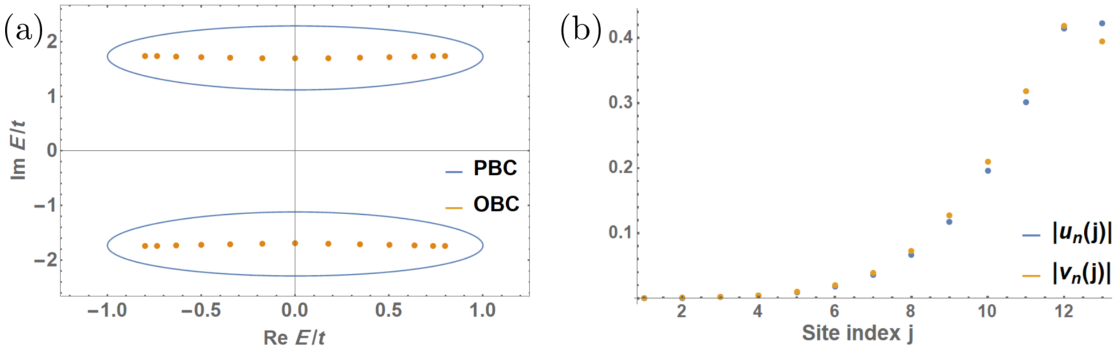

Figure 3.3: (a) Spectrum of the generalized bosonic Kitaev chain described by the Hamiltonian 3.4.1 for both periodic boundary conditions, a open boundary conditions on a lattice with $N = 13$. All eigenvalues of the finite chain lie "inside" the bulk dispersion, and consequently all eigenstates are localized. (b) Unnormalized particle $u_n(j)$ and hole $v_n(j)$ (see Eqs. (3.2.3-3.2.2)) part of the wavefunction for a given eigenstate for the same parameters as in (a). One can easily see that the wavefunctions are localized to one end of the chain, in accordance with the analysis presented in the main text. All other eigenstates are also localized (half to the left, half to the right). Parameters: $\omega_0 = t, \Delta = \nu = 0.5t, \phi = \frac{\pi}{2}$, and $\theta = 0$

we find that a the conclusion holds for a system of finite extent. Indeed our original bosonic Kitaev chain, where only t, Δ and $\phi = \frac{\pi}{2}$ were non-zero, certainly has a non-trivial winding number associated to it. This is already apparent from Fig. 3.1; the energies of the finite-sized system all lie inside the curve drawn out by the bulk energies and, consequently, all eigenstates are localized. In Fig. 3.3 we numerically compute the energies and eigenstates of for a different set of parameters. There too, we observe a localization of all eigenstates which accompany energies that lie within the complex bulk bands.

4

Entanglement Properties

We now consider the ability of our bosonic Kitaev chain to produce entangled photons. While entanglement is a generic feature of bosonic amplifiers, our system has unique features. The local squeezing transformation used to bring the model to particle conserving form has two attractive properties. It renders the problem exactly solvable while also making the nature of both the intra cavity and output light remarkably transparent. We will use this to our advantage by first studying the steady-state produced by letting simple vacuum noise impinge on each site. Unfortunately, the purity of this steady state is too small to be considered interesting. We then show that a generalized version of our model can be used to create a variety multi-mode entangled states which have been proposed to demonstrate so called "quantum supremacy".

4.1 Steady-State

In quantum optics, one is often interested in the long-term dynamics of a driven dissipative open system. Heuristically, one can imagine that the dissipation will push the system into a state in which the driving and coherence in the Hamiltonian will perfectly balance the loss. Thus, in the long-time limit, the system will relax into this state and have no dynamics. Such a simple picture can sometimes fail, e.g. if there is more than one steady state or if there are so called dark states which do not see the dissipation at all. This will not be the case in this section however; we can then identify the steady-state as the long-time limit of the quantity of interest.

In this section we will consider perhaps the simplest steady state we can imagine. The Hamiltonian describing the coherent dynamics is our bosonic Kitaev chain and the dissipation comes from vacuum noise impinging on each site. Further, we assume that the dissipation rate on each site is equal $\kappa_j = \kappa$. The Langevin-Heisenberg equation of motion in the quadrature basis is

$$\dot{\hat{x}}_j = \frac{\tilde{t}}{2}\left(e^{r}\hat{x}_{j-1} - e^{-r}\hat{x}_{j+1}\right) - \frac{1}{2}\kappa\hat{x}_j - \sqrt{\kappa}\hat{x}_j^{(\mathrm{in})}, \tag{4.1.1}$$

$$\dot{\hat{p}}_j = \frac{\tilde{t}}{2}\left(e^{-r}\hat{p}_{j-1} - e^{r}\hat{p}_{j+1}\right) - \frac{1}{2}\kappa\hat{p}_j - \sqrt{\kappa}\hat{p}_j^{(\mathrm{in})}. \tag{4.1.2}$$

The input noise at each is assumed to be uncorrelated Gaussian white noise with zero mean and accompanying correlators $\langle \hat{a}_i^{(\mathrm{in})}(t)\hat{a}_j^{\dagger(\mathrm{in})}(t')\rangle = \delta_{ij}\delta(t-t')$, $\langle \hat{a}_i^{(\mathrm{in})}(t)\hat{a}_j^{(\mathrm{in})}(t')\rangle = \langle \hat{a}_i^{\dagger(\mathrm{in})}(t)\hat{a}_j^{(\mathrm{in})}(t')\rangle = 0$. By the Gaussian assumption, these correlators completely characterize the statistical properties of the noise.

Since the equations of motion are linear, they can be readily be solved by the use of

Green's functions

$$\hat{x}_j(t) = \sum_{j'} \left(e^{r(j-j')} \tilde{G}_0^R[j,j';t]\hat{x}_{j'} + \sqrt{\kappa} e^{r(j-j')} \int_0^t dt' \tilde{G}_0^R[j,j';t-t']\hat{x}_{j'}^{(\text{in})}(t') \right) \tag{4.1.3}$$

$$\hat{p}_j(t) = \sum_{j'} \left(e^{-r(j-j')} \tilde{G}_0^R[j,j';t]\hat{p}_{j'} + \sqrt{\kappa} e^{-r(j-j')} \int_0^t dt' \tilde{G}_0^R[j,j';t-t']\hat{p}_{j'}^{(\text{in})}(t') \right) \tag{4.1.4}$$

where $\tilde{G}_0^R[j,j';t]$ is the retarded Green's function of a particle conserving tight-biding chain with hopping $i\tilde{t}$ and on-site decay rate κ (see Eqs. (2.2.1)-(2.2.2)). Due to the Gaussian nature of the noise, it follows that any state of our system will also be Gaussian. That is, all information about the system's correlations is determined by the $2N \times 2N$ symmetrically ordered covariance matrix $\mathbf{V}$ defined via $V_{jj'} = \frac{1}{2}\langle \Delta\hat{\xi}_j \Delta\hat{\xi}_{j'} + \Delta\hat{\xi}_{j'} \Delta\hat{\xi}_j \rangle$ with $\Delta\hat{\xi}_j = \hat{\xi}_j - \langle \hat{\xi}_j \rangle$ and $\hat{\vec{\xi}} = (\hat{x}_1, \hat{p}_1, \ldots, \hat{x}_N, \hat{p}_N)$. Note that, in our case, the first moments of all operators $\hat{x}_j(t)$ and $\hat{p}_j(t)$ vanish. One can easily find the equal time correlators, and subsequently the $t \to \infty$ correlators, using Eqs. (4.1.3)-(4.1.4). We leave the gory details to Appendix. B and cite the final result

$$\langle \hat{x}_i(\infty)\hat{x}_j(\infty)\rangle = \frac{\kappa i^{i+j}}{2} \left(\frac{2}{N+1}\right)^2 \sum_{j',n,m} e^{r(i+j-2j')} \frac{(-1)^{j'} \sin(k_n j') \sin(k_n i) \sin(k_m j') \sin(k_m j)}{i(E_n + E_m) + \kappa} \tag{4.1.5}$$

$$\langle \hat{p}_i(\infty)\hat{p}_j(\infty)\rangle = \frac{\kappa i^{i+j}}{2} \left(\frac{2}{N+1}\right)^2 \sum_{j',n,m} e^{-r(i+j-2j')} \frac{(-1)^{j'} \sin(k_n j') \sin(k_n i) \sin(k_m j') \sin(k_m j)}{i(E_n + E_m) + \kappa} \tag{4.1.6}$$

$$\frac{1}{2}\langle \hat{x}_i(t)\hat{p}_j(t) + \hat{p}_j(t)\hat{x}_i(t)\rangle = 0 \tag{4.1.7}$$

The last equation follows from the dynamical independence of x and p. Now that we have all relevant correlators, we are in principle ready to examine the entanglement properties of our steady state.

However before doing so, let us recall that each lattice site is coupled to a dissipative bath at a rate determined by the coupling strength κ. Thus, we will have photon flux leaving the various cavities into the bath, which are now entangled. The intracavity states, which is what we are interested in, will then generically be a mixed state. If we want to use the steady-state of our bosonic Kitaev chain as an entanglement resource, ideally we would want our state to be pure. If not, our state is a statistical mixture of several quantum states which necessarily must be described by some density matrix $\hat{\rho}$. The purity μ of a density matrix takes a very simple form for Gaussian states for N bosonic modes [9]

$$\mu = \mathrm{tr}\hat{\rho}^2 = \frac{1}{2^N\sqrt{\det \mathbf{V}}} \tag{4.1.8}$$

The purity of a pure state is, as one would imagine, one. Heuristically, a small value of the purity indicates that the state is a stastical mixture of a large number of quantum states; any quantum information protocol would then be inefficient if performed with any such state.

Unfortunately, we find here that the purity of the bosonic Kiatev chain is quite small and therefore, not a useful resource for entanglement. In Fig. 4.1 we plot the purity as a function of the parametric drive term Δ for a chain with $N = 13$ sites and $\kappa = 10^{-3}t$. At $\Delta = 0$ we see that the system is in a pure state, namely the vacuum. There is no coherent addition of photons to balance the dissipation and, in the long-time limit, the system relaxes into a state with no photons in any of the cavities. As we increase the driving term Δ we see that we very quickly become impure. We can therefore conclude that the steady state of the bosonic Kitaev chain is not a good resource of intracavity

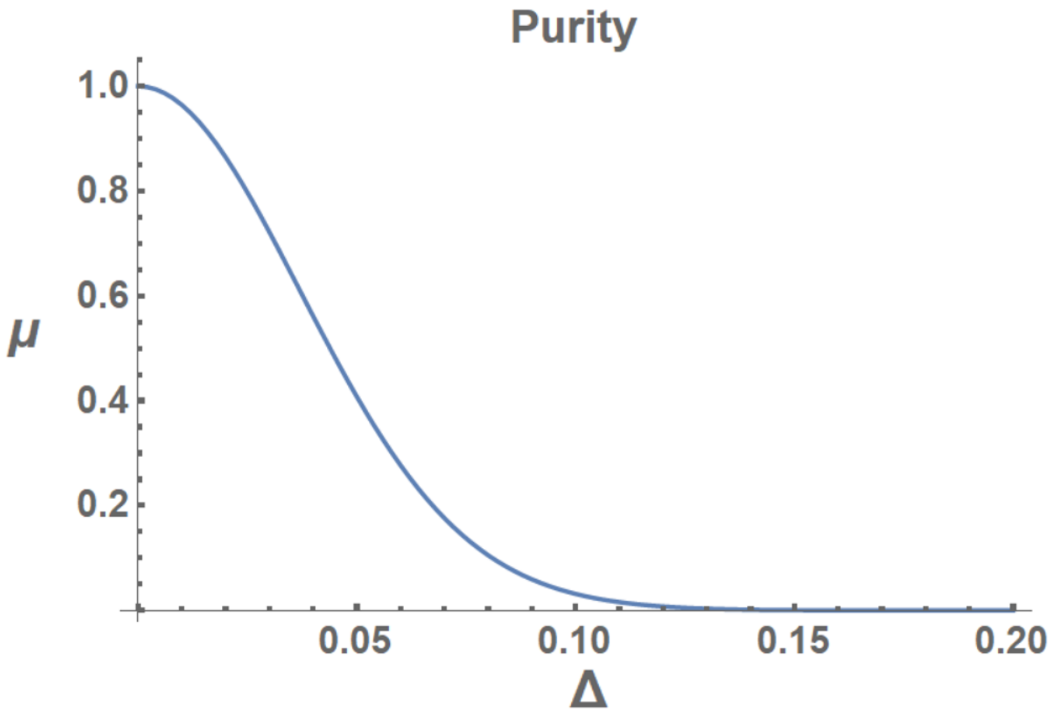

Figure 4.1: Purity μ of the steady state as a function of the drive amplitude Δ. When $\Delta = 0$ the steady state is the collective vacuum of all the cavities and the state is manifestly pure. As we increase Δ, the purity decays exponentially. Thus, the intracavity light in the steady state is not a good source of entanglement.

entanglement.

4.2 Multi-Partite Entanglement

We've just seen that the steady-state of the bosonic Kitaev chain is not an ideal producer of entanglement. This follows immediately by considering the purity; it was too small to be considered useful. Physically, the fact that our state is mixed is because we have not kept track of the photons emerging from our system. To overcome this issue, we may consider using outgoing states of light as an entanglement resource. The necessary machinery required for such a task has already been developed; using input-output theory we've completely characterized the outgoing states of light using the scattering matrix.

To be more concrete, let us consider a set of $M \leq N$ input-output waveguides coupled to the sites in our lattice where, as before, N is the number of lattice sites. As we've seen in the previous section, even if vacuum noise is incident on each site, there will be a non-zero number of photons in the light emerging from the waveguides. Further, such light has a remarkably transparent form; it consists of sending in squeezed light in a beam-splitter network, and then again squeezing the light at the output. A schematic of the setup is depicted in Fig. 4.2 and follows immediately from Eqs (2.3.2)-(2.3.3). First, one prepares M squeezed states with squeezing parameter $R_j = rj$ (see Eq. (2.1.3)) in the waveguide coupled to site j. At this point, the photons in waveguide j do no exhibit any correlations with photons in other waveguides j'. The photons are then subsequently sent into an effective beam splitter network, described by a $M \times M$ unitary matrix K; this is just the scattering matrix of a particle conserving tight-binding model with hopping amplitude $i\tilde{t}$ and couplings κ_j. Finally, one performs a local anti-squeezing transformation of the light at the output, yet another completely local operation. As such, it does not affect the entanglement properties of the output light.

The states depicted in Fig. 4.2 have recently received attention as potentially useful in demonstrating "quantum supremacy: the idea that a quantum mechanical system can compute something that is classically difficult to do. In particular, these states can be used to compute the molecular vibronic spectra [19], as well as solving classically-hard graph-theoretical problems [20]. We note that normally, producing such states is experimentally challenging. One first has to produce M squeezed states, then transporting and injecting them with high efficiency into a beam-splitter network, a non-trivial task. The bosonic Kitaev chain thus circumvents this problem by generating all the squeezing locally.

If one wanted to use our system for such applications, we would ideally like to have full control over both the squeezing parameters R_j and unitary matrix K describing the beam-splitter network. We can achieve the former by letting the hopping amplitude and

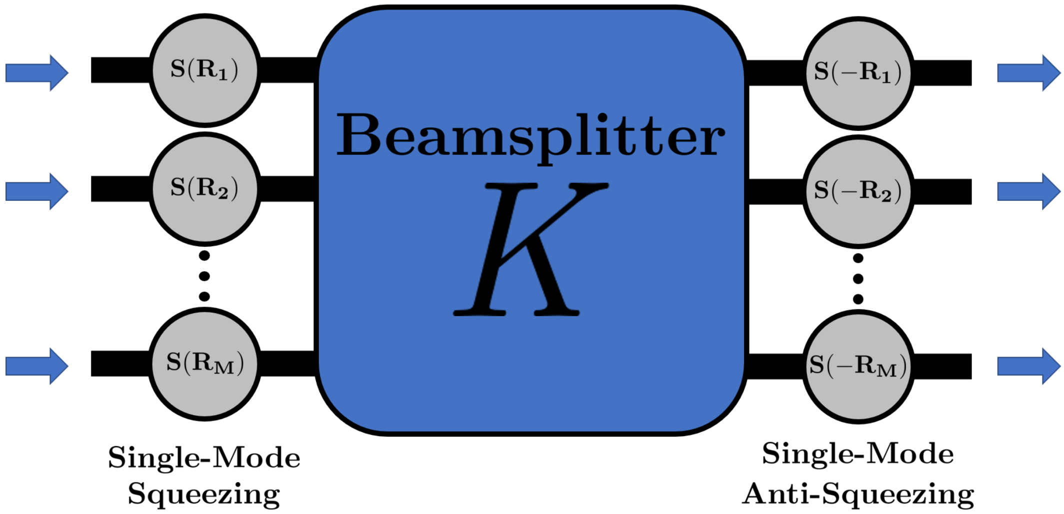

Figure 4.2: Schematic showing an equivalent depiction of scattering off our lattice with M input-output waveguides coupled to $M \leq N$ arbitrary sites. Input states in each waveguide are first locally squeezed (squeeze parameters R_j). They then pass through a beam-splitter network, and are then finally locally anti-squeezed at the outputs. Crucially, the squeeze parameters R_j and beam-splitter unitary matrix K have a direct and simple relation to the system Hamiltonian. In particular, K is the unitary of a simple tight-binding model (see Eqs. (4.2.6-4.2.7)).

parametric drive vary from bond to bond $t \to t_j$, $\Delta \to \Delta_j$. Crucially, we require that the phase of the hopping amplitude remain the same, i.e. it is purely imaginary. The corresponding Hamiltonian of this generalized bosonic Kitaev chain is

$$\hat{H}_B \equiv \frac{1}{2}\sum_{j=1}^{N-1}\left(it_j\hat{a}^\dagger_{j+1}\hat{a}_j + i\Delta_j\hat{a}^\dagger_{j+1}\hat{a}^\dagger_j + h.c.\right) \tag{4.2.1}$$

$$= \frac{1}{2}\sum_{j=1}^{N}\left(-(t_j - \Delta_j)\hat{x}_{j+1}\hat{p}_j + (t_j + \Delta +_j)\hat{p}_{j+1}\hat{x}_j)\right) \tag{4.2.2}$$

Although we do not expect to be able to diagonalize this Hamiltonian as before, we would still like to characterize when instability occurs. Recall from our previous discussion that, for the translationally invariant clean Hamiltonian, stability was guaranteed by the fact that the x and p quadratures were dynamically decoupled in conjunction with the chiral nature of the amplification and de-amplification. Yet both of those features are present even without translational invariance. Thus, as we will now show, stability is achieved if the tunneling matrix elements are larger than the parametric drive terms.

More explicitly if we assume that $t_j > \Delta_j$ for all j and define

$$e^{2r_j} = \frac{t_j + \Delta_j}{t_j - \Delta_j}, \quad R_j = \sum_{m=0}^{j-1} r_m, \tag{4.2.3}$$

with r_0 an arbitrary real number, we can make a local position-dependent squeezing transformation:

$$\hat{U}\hat{x}_j\hat{U}^\dagger = e^{R_j}\hat{\tilde{x}}_j, \qquad \hat{U}\hat{p}_j\hat{U}^\dagger = e^{-R_j}\hat{\tilde{p}}_j \tag{4.2.4}$$

A direct substitution yields

$$\hat{U}\hat{H}_{B'}\hat{U}^\dagger = \frac{1}{2}\sum_j \left(i\tilde{t}_j\hat{\tilde{a}}^\dagger_{j+1}\hat{\tilde{a}}_j + h.c.\right), \tag{4.2.5}$$

with $\tilde{t}_j = \sqrt{t_j^2 - \Delta_j^2}$.

Thus, in the case where $t_j > \Delta_j$ for all j, $\hat{H}_{B'}$ is unitarily equivalent to a particle conserving tight-binding chain with a spatially varying tunnel matrix element $i\tilde{t}_j$. This mapping also implies a simple form for the scattering matrices that corresponds to Fig. 4.2:

$$s^x_{jj'}[\omega] = e^{R_j - R_{j'}}\tilde{s}_{jj'}[\omega], \tag{4.2.6}$$

$$s^p_{jj'}[\omega] = e^{-(R_j - R_{j'})}\tilde{s}_{jj'}[\omega] \tag{4.2.7}$$

where now $\tilde{s}_{jj'}[\omega]$ is the scattering matrix of an N-site tight binding chain with hopping matrix elements $i\tilde{t}_j$ and on-site decay rates κ_j. Therefore, experimental control over t_j

and Δ_j allows one to realized a large class of multi-mode entangled states.

5

Conclusion and outlook

The original purpose of this thesis was deceptively simple; finding and characterizing the correct analogue of the celebrated Kitaev chain in the bosonic setting. Our starting point was replacing the exoctic Majorana particles in Kitaev's model with the well known quadrature operators $\hat{x}$ and $\hat{p}$ for bosons, the rational being that all the interesting physics in the Kitaev chain come from the Majorana pairing structure. Despite the formally similar Hamiltonians, the two problems nearly nonidentical, a consequence of particle statistics. In our model, photonic wavepackets propagate and are amplified in a manner that depends on it's phase. Further, the bosonic Kitaev chain exhibits sensitivity to boundary conditions that is much stronger than any conventional condensed matter system. The addition of boundaries not only localizes all states to the edge, but also makes these modes dynamically stable. These features can be tentatively attributed to a non-trivial winding of the bulk spectrum in the complex plane, which is only possible in a driven-dissipative system. Our system is not only of fundamental interest, but could also serve as a useful resource for quantum computing. While the steady-state is too impure to be of interest, a generalized version of the bosonic Kitaev chain can be used to prepare a large class of multi-mode entangled states that have received recent attention in the literature.

In terms of outlook, the physics discussed in this thesis perhaps raises more questions that it answers. We have made a surprising connection between the Majorana modes and the bosonic quadrature operators; one can only wonder if this correspondence can be taken further. Namely, the classification of fermionic topological band structure can be understood entirely in terms of Majorana fermions [21]. It is only nature to ask if the quadrature operators play a similar role in the bosonic case. Finally, the role of real photon-photon interactions in this setting would be extremely interesting.

A

Scattering matrix of a regular tight-binding chain

For completeness, here we derive the expression of the photon scattering matrix of a regular tight-binding chain $\tilde{s}_{jj'}[\omega]$, from which we immediately obtain the quadrature scattering matrices, c.f. Eqs (2.3.2)-(2.3.3). The first step is to compute the Green's function $\tilde{\mathbf{G}}_0[\omega]$ of the unperturbed system, i.e. without the spatially dependent loss. By definition,

$$\tilde{\mathbf{G}}_0[\omega] = \Big((\omega + i\frac{\kappa}{2})\mathbf{1} - \mathbf{H}\Big)^{-1} \tag{A.1}$$

where κ is the uniform on-site decay rate and $\mathbf{H}$ is the single particle Hamiltonian which, in real space, has matrix elements (c.f. Eq. (2.1.5))

$$H_{ij} = i\frac{\tilde{t}}{2}\delta_{i,j+1} - i\frac{\tilde{t}}{2}\delta_{i,j-1}. \tag{A.2}$$

Note that we could make a local gauge transformation to make the Hamiltonian matrix $\mathbf{H}$ real valued. However, this transformation would also alter the scattering matrix, and we therefore choose to keep the imaginary phase factors in the definition of the Hamiltonian. With Eq. (A.1) in combination with Eq. (A.2), one easily verifies that the Green's function for a finite chain of N sites is

$$\tilde{G}_0[j,j';\omega] = i^{j-j'} \frac{2\sin\left(q[\omega]\min(j,j')\right)\sin\left(q[\omega](N+1-\max(j,j'))\right)}{\tilde{t}\sin\left(q[\omega]\right)\sin\left(q[\omega](N+1)\right)} \tag{A.3}$$

where $q[\omega]$ is the complex wavevector satisfying the dispersion

$$\omega + i\frac{\kappa}{2} - \tilde{t}\cos(q[\omega]) = 0. \tag{A.4}$$

The introduction of spatially dependent loss κ_j introduces an effective imaginary potential $\mathbf{V}$ at each lattice site. In real space it has matrix elements

$$V_{ij} = -i\frac{\kappa_j}{2}\delta_{ij}. \tag{A.5}$$

The full Green's function $\tilde{\mathbf{G}}[\omega]$ is given by Dyson's equation

$$\tilde{\mathbf{G}}[\omega] = \tilde{\mathbf{G}}_0[\omega] + \tilde{\mathbf{G}}_0[\omega]\mathbf{V}\tilde{\mathbf{G}}[\omega] = \frac{1}{\mathbf{1} - \tilde{\mathbf{G}}_0[\omega]\mathbf{V}}\tilde{\mathbf{G}}_0[\omega]. \tag{A.6}$$

Standard input-output theory [10, 11] then gives a simple relation between the scattering matrix and the Green's function

$$s_{jj'}[\omega] = \delta_{jj'} - i\sqrt{\kappa_j\kappa_{j'}}\tilde{G}[j,j';\omega] \tag{A.7}$$

B

Steady-State Correlators

In this appendix we derive the steady state correlators of our bosonic Kitaev chain in the presence of uniform damping κ on each site. It is obvious that there are no dark states, i.e. states which are unaware of the dissipation and that the steady state will be unique. We may then identify the steady state correlators $\langle \hat{x}_i \hat{x}_j \rangle_{\text{ss}}$ and $\langle \hat{p}_i \hat{p}_j \rangle_{\text{ss}}$ as the $t \to \infty$ limit of the equal time correlators $\langle \hat{x}_i(t) \hat{x}_j(t) \rangle$ and $\langle \hat{p}_i(t) \hat{p}_j(t) \rangle$ respectively (two-point correlators involving both $\hat{x}$ and $\hat{p}$ vanish since they are dynamically decoupled). Recall that in the main text, we had found the solution to $\hat{x}_i(t)$ and $\hat{p}_i(t)$ using the Green's function technique

$$\hat{x}_j(t) = \sum_{j'} \left(e^{r(j-j')} \tilde{G}_0^R[j,j';t] \hat{x}_{j'} + \sqrt{\kappa} e^{r(j-j')} \int_0^t dt' \tilde{G}_0^R[j,j';t-t'] \hat{x}_{j'}^{(\text{in})}(t') \right) \tag{B.1}$$

$$\hat{p}_j(t) = \sum_{j'} \left(e^{-r(j-j')} \tilde{G}_0^R[j,j';t] \hat{p}_{j'} + \sqrt{\kappa} e^{-r(j-j')} \int_0^t dt' \tilde{G}_0^R[j,j';t-t'] \hat{p}_{j'}^{(\text{in})}(t') \right) \tag{B.2}$$

with $\tilde{G}_0^R[j,j';t]$ the Green's function for a particle conserving tight-binding model with imaginary $i\tilde{t}$. Thankfully, we've already found the eigenstates $\psi_n(j)$ and energies E_n of the Hamiltonian: they are simple standing waves

$$\psi_n(j) = \sqrt{\frac{2}{N+1}} i^j \sin(k_n j), \qquad , E_n = \tilde{t}\cos(k_n) \qquad k_n = \frac{n\pi}{N+1} \tag{B.3}$$

The retarded Green's function can then be readily found by using the spectral decomposition

$$\begin{aligned} \tilde{G}_0^R[j,j';t] &= \sum_n \psi_n(j)\psi_n(j')^* e^{-iE_n t - \frac{\kappa}{2}t} \\ &= \frac{2i^{j-j'}}{N+1}\sum_n \sin(k_n j)\sin(k_n j')\, e^{-iE_n t} e^{-\frac{\kappa}{2}t} \end{aligned} \tag{B.4}$$

We are now in a position to compute the relevant correlators.

Before doing so, we first notice two things which will simplify said correlators. The first is that it is only necessary to compute either $\langle \hat{x}_i \hat{x}_j\rangle_{\mathrm{ss}}$; the other correlator $\langle \hat{p}_i \hat{p}_j\rangle_{\mathrm{ss}}$ can be found by changing the sign of the squeezing parameter $r \to -r$. The second thing to note is that $\hat{x}_i(t)$ can be decomposed into two terms. The first corresponds to the free evolution of the cavity modes, whereas the second includes the effects of the dissipative bath on each site. In the $t \to \infty$ limit, the former will vanish due to the damping induced by the coupling to the baths. Thus, using Eq. (B.1) and the cavity correlators $\langle \hat{x}_i^{(\mathrm{in})}(t)\hat{x}_j^{(\mathrm{in})}(t')\rangle = \delta_{ij}\delta(t-t')/2$, we obtain

$$\begin{aligned} \langle \hat{x}_i(t)\hat{x}_j(t)\rangle &= \kappa \sum_{j',j''} e^{r(i-j'+j-j'')} \int_0^t \int_0^t dt' dt'' \tilde{G}_0^R[i,j',t-t']\tilde{G}_0^R[j,j'',t-t'']\langle \hat{x}_{j'}^{(\mathrm{in})}(t')\hat{x}_{j''}^{(\mathrm{in})}(t'')\rangle \\ &= \frac{\kappa}{2}\sum_{j'}\left(e^{r(i+j-2j')}\int_0^t dt' \tilde{G}_0^R[i,j',t-t']\tilde{G}_0^R[j,j',t-t']\right) \end{aligned} \tag{B.5}$$

Plugging Eq. (B.4) into the equation above and performing the elementary integration leads to the result quoted in the main text

$$\langle \hat{x}_i(\infty)\hat{x}_j(\infty)\rangle = \frac{\kappa i^{i+j}}{2}\left(\frac{2}{N+1}\right)^2 \sum_{j',n,m} e^{r(i+j-2j')}\frac{(-1)^{j'}\sin(k_n j')\sin(k_n i)\sin(k_m j')\sin(k_m j)}{i(E_n+E_m)+\kappa} \tag{B.6}$$

Bibliography

[1] A. Kitaev, Phys. Usp. **44**, 131 (2001).

[2] J. Alicea, Reports on Progress in Physics **75**, 076501 (2012).

[3] C. L. Kane and E. J. Mele, Phys. Rev. Lett. **95**, 226801 (2005).

[4] C. L. Kane and E. J. Mele, Phys. Rev. Lett. **95**, 146802 (2005).

[5] M. Aspelmeyer, T. J. Kippenberg, and F. Marquardt, Rev. Mod. Phys. **86**, 1391–1452 (2014).

[6] G. Wendin, Reports on Progress in Physics **80**, 106001 (2012).

[7] C. Leroux, L. C. G. Govia, and A. A. Clerk, Phys. Rev. Lett. **120**, 093602 (2018).

[8] C. Gerry and P. Knight (Cambridge University Press, 2004).

[9] S. L. Braunstein and P. van Loock, Rev. Mod. Phys. **77**, 513–577 (2005).

[10] A. A. Clerk, M. H. Devoret, S. M. Girvin, F. Marquardt, and R. J. Schoelkopf, Rev. Mod. Phys. **82**, 1155 (2010).

[11] C. W. Gardiner and P. Zoller (Springer, Berlin, 2000).

[12] V. Peano, M. Houde, C. Brendel, F. Marquardt, and A. A. Clerk, Nat. Commun. **7**, 10779 (2016).

[13] V. Peano, M. Houde, F. Marquardt, and A. A. Clerk, Phys. Rev. X **6**, 041026 (2016).

[14] R. Shindou, R. Matsumoto, S. Murakami, and J.-i. Ohe, Phys. Rev. B **87**, 174427 (2013).

[15] G Engelhardt and T Brandes, Phys. Rev. A **91**, 053621 (2015).

[16] G Engelhardt, M Benito, G Platero, and T Brandes, Phys. Rev. Lett. **117**, 045302 (2016).

[17] Y. Xiong, arXiv:1705.06039v1 (2017).

[18] Z. Gong, Y. Ashida, K. Kawabata, K. Takasan, S. Higashikawa, and M. Ueda, arXiv:1802.07964v1 (2018).

[19] J. Huh, G. G. Guerreschi, B. Peropadre, J. R. McClean, and A. Aspuru-Guzik, Nat. Photon. **9**, 615 (2015).

[20] K. Brádler, P.-L. Dallaire-Demers, P. Rebentrost, D. Su, and C. Weedbrook, arXiV:1712.06729v1 (2017).

[21] A. Kitaev, AIP Conference Proceedings **1134**, 22–30 (2009).

[22] N. E. Frattini, U. Vool, S. Shankar, A. Narla, K. M. Sliwa, and M. H. Devoret, Appl. Phys. Lett. **110**, 222603 (2017).

[23] B. Abdo, A. Kamal, and M. Devoret, Phys. Rev. B **87**, 014508 (2013).

[24] N. Hatano and D. R. Nelson, Phys. Rev. B **56**, 8651–8673 (1997).

[25] C.-E. Bardyn, T. Karzig, G. Refael, and T. C. H. Liew, Phys. Rev. B **93**, 020502 (2016).

[26] C. E. Bardyn and A Imamoglu, Phys. Rev. Lett. **109**, 253606 (2012).

[27] G. Vidal and R. F. Werner, Phys. Rev. A **65**, 032314 (2002).

[28] C. S. Hamilton, R. Kruse, L. Sansoni, S. Barkhofen, C. Silberhorn, and I. Jex, Phys. Rev. Lett. **119**, 170501 (2017).

[29] C. Beenakker, Ann. Rev. Cond. Mat. Phys. **4**, 113–136 (2013).

[30] S. Das Sarma, M. Freedman, and C. Nayak, npj Quant. Inf. **1**, 15001 (2015).

[31] T. Karzig, Y. Oreg, G. Refael, and M. H. Freedman, Phys. Rev. X **6**, 031019 (2016).

[32] Y. Oreg, G. Refael, and F. von Oppen, Phys. Rev. Lett. **105**, 177002 (2010).

[33] S. L. Braunstein, Phys. Rev. A **71**, 10–4 (2005).

[34] S. Aaronson and A. Arkhipov, Theory Comput. **9**, 143 (2013).

[35] B. Galilo, D. K. K. Lee, and R. Barnett, Phys. Rev. Lett. **115**, 245302 (2015).

[36] R. Barnett, Phys. Rev. A **88**, 063631 (2013).

[37] J. Maciejko, T. L. Hughes, and S.-C. Zhang, Annu. Rev. Condens. Matter Phys. **2**, 31–53 (2011).